RESEARCH PAPER

Design, Characterization, and Colon-Specific Delivery of Berberrubine-Embedded pH-Responsive Polymeric Hydrogel System for Targeted Intervention in Crohn's Disease

Rangu Nirmala[1], Palash Chandra Biswas[2], D. Suresh[3*], Mohd Wamiq[4], Sarvar Jahan[5], Momin Zarina Md. Najeeb[6], Dilip Kumar Roy[7], V. Sandhya[8]

[1]Associate Professor, Sri Ranganayaka Swamy College of Pharmacy, Siddipet, Telangana. 502276

[2]Assistant Professor, Netaji Subhas Chandra Bose Institute of Pharmacy, Chakdaha - Bongaon Rd, Roypara, Tatla, Nadia, West Bengal. 741222

[3*]Professor, KMCT College of Pharmaceutical Sciences, Kallanthode, Nitc-Po, Kozhikode, Kerala. 673601. Email: dsureshpdy@gmail.com (Corresponding Author)

[4]Assistant Professor, School of Pharmacy, Mangalayatan University, Aligarh, Uttar Pradesh, India.

[5]Assistant Professor, SAM Global University, Agariya Chopda, Raisen, Madhya Pradesh. 464551

[6]Assistant Professor, Ali Allana College of Pharmacy, Jamia Campus, Molgi Road, Akkalkuwa, Nandurbar, Maharashtra. 425415

[7]Associate Professor, Department of Pharmaceutical Technology, JIS University, 81, Nilgunj Road, Agarpara, North 24 Parganas, Kolkata, West Bengal. 700109

[8]Department of Pharmaceutical Chemistry, Faculty of Pharmacy, Sree Balaji Medical College and Hospital campus, Bharath Institute of Higher Education & Research, Chromepet, Chennai, Tamilnadu.

ABSTRACT

Objective: The present study focused on the design, characterization, and in vitro evaluation of a berberrubine-embedded pH-responsive polymeric hydrogel system for colon-specific delivery aimed at targeted intervention in Crohn's disease. The hydrogel was synthesized using free radical polymerization of methacrylic acid and acrylamide with controlled crosslinking density to achieve pH-triggered swelling behaviour.

Characterization: Drug–polymer compatibility was confirmed through FTIR analysis, demonstrating structural integrity without significant chemical interaction. The optimized formulation (F3) exhibited high encapsulation efficiency (84.6%) and an optimal gel fraction (90.5%), indicating a stable and well-formed polymeric network. Swelling studies revealed minimal expansion in acidic conditions (pH 1.2) and significant swelling at colonic pH (7.4), confirming strong pH responsiveness. In vitro pH-shift dissolution studies demonstrated negligible drug release in gastric conditions followed by enhanced release under simulated colonic conditions.

Kinetic and Safety Analysis: Kinetic modeling indicated that the drug release followed the Korsmeyer–Peppas model with super case-II transport behavior, suggesting polymer relaxation-driven release. Surface morphology analysis showed a porous network architecture supporting diffusion-controlled release. Cytocompatibility assessment confirmed high cell viability, indicating formulation safety.

Conclusion: Overall, the developed hydrogel system represents a promising colon-targeted delivery platform for localized therapy in inflammatory bowel disorders.

Keywords: Berberrubine; Colon-targeted drug delivery; Crohn's disease; pH-responsive hydrogel; Polymer relaxation kinetics; Super case-II transport

How to cite this article: Nirmala R, Biswas PC, Suresh D, Wamiq M, Jahan S, Najeeb MZM, Roy DK, Sandhya V. Design, Characterization, and Colon-Specific Delivery of Berberrubine-Embedded pH-Responsive Polymeric Hydrogel System for Targeted Intervention in Crohn's Disease. Int J Drug Deliv Technol. 2026;16(14s): 444-456. DOI: 10.25258/ijddt.16.14s.47

Source of support: Nil.

Conflict of interest: None

1. Introduction:

Crohn's disease is a chronic, relapsing inflammatory disorder of the gastrointestinal tract characterized by transmural inflammation, ulceration, and progressive tissue damage. It predominantly affects the terminal ileum and colon, leading to symptoms such as abdominal pain, diarrhea, rectal bleeding, weight loss, and impaired quality of life. The pathogenesis of

Crohn's disease involves a complex interplay between genetic susceptibility, immune dysregulation, environmental triggers, and alterations in the intestinal microbiota. Excessive production of pro-inflammatory cytokines, including tumor necrosis factor-α (TNF-α) and interleukin-6 (IL-6), contributes significantly to mucosal injury and sustained inflammation. Despite advances in biologic therapies and immunomodulators, conventional treatment approaches often suffer from systemic side effects, incomplete remission, and high relapse rates, highlighting the need for improved targeted therapeutic strategies (Cockburn *et al.*, 2023; Dolinger *et al.*, 2024; Ozbey *et al.*, 2025; Srinivasan, 2024).

Colon-specific drug delivery systems have emerged as a promising approach for localized treatment of inflammatory bowel diseases. By directing the therapeutic agent specifically to the inflamed colonic region, it is possible to enhance local drug concentration while minimizing systemic exposure and associated adverse effects. Among various targeting strategies, pH-responsive polymeric systems are particularly attractive due to the well-defined pH gradient along the gastrointestinal tract. The stomach exhibits a highly acidic environment (pH ~1–2), the small intestine maintains a near-neutral pH (6–7), and the colon presents a slightly alkaline environment (pH 7–7.5). Exploiting these physiological variations allows for the development of smart delivery systems that remain intact in gastric conditions and release the drug selectively in the colon (Ghosh & Basak, 2025; Mishra *et al.*, 2026; Siddiqui *et al.*, 2025; Singh *et al.*, 2025; Wang *et al.*, 2025; Wu *et al.*, 2024).

Hydrogels are three-dimensional, crosslinked polymeric networks capable of absorbing large quantities of water without dissolving. Their high swelling capacity, biocompatibility, tunable mechanical strength, and responsiveness to environmental stimuli make them suitable carriers for controlled drug delivery. In particular, hydrogels incorporating ionizable functional groups such as carboxylic moieties can exhibit pH-sensitive swelling behaviour. At low pH, these groups remain protonated, resulting in minimal swelling and restricted drug diffusion. In contrast, at higher pH, ionization leads to electrostatic repulsion within the polymer network, causing expansion and enhanced drug release (Evers & Alexander, 2025; Fang *et al.*, 2025; Manna *et al.*, 2024; Verma *et al.*, 2023). Berberrubine, a bioactive isoquinoline alkaloid derivative, has attracted attention due to its reported anti-inflammatory and immunomodulatory properties. Its therapeutic potential in inflammatory conditions makes it a promising candidate for localized delivery in Crohn's disease. However, systemic administration may limit its effectiveness due to variable bioavailability and potential off-target effects. Encapsulation within a pH-responsive hydrogel matrix may overcome these limitations by ensuring site-specific release and sustained therapeutic action (Ahalya *et al.*, 2026; Chu *et al.*, 2025; Jana *et al.*, 2025; Jiang *et al.*, 2026; Saroj *et al.*, 2026; Seng *et al.*, 2026; Xiao *et al.*, 2025).

In this context, the present study aimed to design and evaluate a berberrubine-loaded pH-responsive polymeric hydrogel system for colon-targeted drug delivery. The formulation was optimized based on physicochemical characterization, swelling behaviour, in vitro release kinetics, surface morphology, and cytocompatibility. By integrating polymer science with targeted delivery principles, this investigation sought to establish a rational and efficient platform for localized intervention in Crohn's disease.

2. Materials and Methods:

2.1 Materials:

Berberrubine (≥98% purity) was obtained from a certified phytochemical supplier and used without further purification. Methacrylic acid (MAA) and acrylamide (AAm) were selected as pH-responsive monomer components for hydrogel synthesis. N,N′-methylenebisacrylamide (MBA) served as the crosslinking agent, while ammonium persulfate (APS) and N,N,N′,N′-tetramethylethylenediamine (TEMED) were employed as the initiator–accelerator system for free radical polymerization. Phosphate buffer components, sodium chloride, potassium dihydrogen phosphate, sodium hydroxide, and hydrochloric acid were of analytical grade and used for preparing dissolution media of different pH values (1.2, 6.8, and 7.4). All solvents were of analytical reagent grade, and distilled water was used throughout the experimental procedures. The selection of methacrylic acid was based on its ionizable carboxylic functional groups, which exhibit minimal ionization in acidic gastric pH but undergo significant ionization at colonic pH, thereby enabling pH-triggered swelling and controlled drug release. All chemicals were stored under recommended storage conditions to preserve stability and prevent degradation.

2.2 Formulation Design and Experimental Strategy:

The hydrogel formulations were designed to achieve colon-specific drug delivery through pH-dependent swelling and controlled drug release behaviour. A series of five formulations (F1–F5) were developed by

varying the concentration of methacrylic acid and crosslinking density while maintaining a constant drug load. The formulation strategy focused on optimizing polymer composition to achieve minimal swelling and drug release in acidic conditions (pH 1.2), moderate response at intestinal pH (6.8), and maximum swelling and release at colonic pH (7.4) (Asamoah *et al.*, 2025; Ashfaq *et al.*, 2025; Ding *et al.*, 2025; Eltabeeb *et al.*, 2025; Guo *et al.*, 2025; Guzenko *et al.*, 2025; Hanan *et al.*, 2025). The crosslinking density was carefully adjusted to balance mechanical strength and diffusion characteristics. Lower crosslinking was expected to enhance swelling but reduce structural integrity, whereas excessive crosslinking could restrict swelling and delay drug release. Therefore, systematic variation of polymer-to-crosslinker ratio was implemented to identify an optimized hydrogel composition suitable for colon-targeted intervention in Crohn's disease. All formulations were prepared in triplicate to ensure reproducibility and minimize experimental variation.

2.3 Preparation of Berberrubine-Embedded pH-Responsive Hydrogel:

Berberrubine-embedded hydrogels were synthesized using a free radical polymerization technique. Initially, the required quantity of methacrylic acid and acrylamide was dissolved in distilled water under continuous magnetic stirring at room temperature until a homogeneous solution was obtained. The calculated amount of berberrubine was then dispersed in the monomer solution under constant stirring to ensure uniform distribution throughout the polymeric matrix (Asamoah *et al.*, 2025; Ashfaq *et al.*, 2025; Ding *et al.*, 2025; Eltabeeb *et al.*, 2025; Guo *et al.*, 2025; Guzenko *et al.*, 2025; Hanan *et al.*, 2025). Subsequently, ammonium persulfate was added as the free radical initiator, followed by the addition of N,N′-methylenebisacrylamide as the crosslinking agent. Finally, TEMED was introduced to accelerate the polymerization process. The reaction mixture was immediately transferred into pre-lubricated cylindrical glass molds to allow in situ polymerization. The polymerization process was allowed to proceed undisturbed at room temperature for 24 hours to ensure complete network formation (Asamoah *et al.*, 2025; Ashfaq *et al.*, 2025; Ding *et al.*, 2025; Eltabeeb *et al.*, 2025; Guo *et al.*, 2025; Guzenko *et al.*, 2025; Hanan *et al.*, 2025). After polymerization, the formed hydrogel rods were carefully removed from the molds and cut into uniform discs of predetermined thickness. The discs were repeatedly washed with distilled water to remove any unreacted monomers and residual initiator. The washed hydrogels were then dried in a hot air oven at 40°C until a constant weight was achieved. Dried hydrogel samples were stored in airtight containers for further characterization.

2.4 Preformulation and Drug–Polymer Compatibility Studies:

Prior to formulation development, preformulation investigations were carried out to evaluate the physicochemical compatibility between berberrubine and the selected polymeric components. Fourier Transform Infrared (FTIR) spectroscopy was employed to assess potential chemical interactions between the drug and excipients. Pure berberrubine, individual polymers, and the optimized hydrogel formulation were subjected to FTIR analysis using a spectrophotometer in the range of 4000–400 cm^{-1}. Samples were prepared by the potassium bromide (KBr) pellet method. The characteristic peaks corresponding to functional groups of berberrubine were carefully analyzed and compared with spectra obtained from the polymer and the final hydrogel formulation. Any significant shift, disappearance, or formation of new peaks was evaluated to determine possible drug–polymer interactions. In addition to FTIR analysis, preliminary solubility evaluation of berberrubine was conducted in various media including distilled water and phosphate buffers of pH 1.2, 6.8, and 7.4 to determine its dissolution behavior under gastrointestinal conditions. The solubility study assisted in selecting appropriate analytical methods and ensuring sink conditions during in vitro release experiments (Asamoah *et al.*, 2025; Ashfaq *et al.*, 2025; Ding *et al.*, 2025; Eltabeeb *et al.*, 2025; Guo *et al.*, 2025; Guzenko *et al.*, 2025; Hanan *et al.*, 2025).

2.5 Determination of Drug Loading and Encapsulation Efficiency:

The drug loading capacity and encapsulation efficiency of the prepared hydrogel formulations were determined to quantify the amount of berberrubine successfully incorporated into the polymeric matrix. Accurately weighed dried hydrogel samples were crushed into fine particles and immersed in a known volume of phosphate buffer (pH 7.4). The mixture was stirred continuously to ensure complete extraction of the drug from the hydrogel network. After sufficient extraction time, the solution was filtered to remove polymeric debris. The filtrate was analyzed using UV–Visible spectrophotometry at the predetermined wavelength corresponding to the maximum absorbance (λmax) of berberrubine. A previously constructed calibration curve was used to determine the drug concentration. Encapsulation efficiency was calculated as the ratio of the experimentally determined drug content to the

theoretical drug content incorporated during formulation preparation. Drug loading percentage was also calculated to evaluate the proportion of drug present relative to the total weight of the hydrogel. All measurements were performed in triplicate to ensure reproducibility and accuracy (Asamoah *et al.*, 2025; Ashfaq *et al.*, 2025; Ding *et al.*, 2025; Eltabeeb *et al.*, 2025; Guo *et al.*, 2025; Guzenko *et al.*, 2025; Hanan *et al.*, 2025).

2.6 Gel Fraction and Network Integrity Analysis:

The gel fraction of the hydrogel formulations was determined to assess the extent of crosslinking and network stability. Dried hydrogel samples were accurately weighed and immersed in distilled water for 24 hours at room temperature to allow the extraction of soluble, non-crosslinked polymer fractions. After the extraction period, the samples were removed, dried again at 40°C until constant weight, and reweighed. The gel fraction was calculated as the percentage ratio of the final dried weight to the initial dried weight of the hydrogel sample. A higher gel fraction indicated greater crosslinking density and improved structural integrity of the hydrogel network. This parameter was critical in determining the mechanical robustness and diffusion characteristics of the hydrogel system (Ahalya *et al.*, 2026; Asamoah *et al.*, 2025; Ashfaq *et al.*, 2025; Ding *et al.*, 2025; Eltabeeb *et al.*, 2025; Guo *et al.*, 2025; Guzenko *et al.*, 2025; Hanan *et al.*, 2025).

2.7 Swelling Studies:

The swelling behaviour of the hydrogel formulations was evaluated to understand their pH-responsive characteristics and suitability for colon-specific drug delivery. Dried hydrogel discs of uniform dimensions were accurately weighed and immersed separately in simulated gastric fluid (pH 1.2), simulated intestinal fluid (pH 6.8), and simulated colonic fluid (pH 7.4) at 37 ± 0.5°C. At predetermined time intervals, the hydrogel discs were removed, gently blotted with filter paper to eliminate excess surface moisture, and weighed immediately. The swelling index was calculated using the difference between swollen weight and initial dry weight. The study was continued until equilibrium swelling was achieved. The swelling behaviour was expected to be minimal at pH 1.2 due to limited ionization of carboxylic groups and significantly higher at pH 7.4 due to increased ionization and electrostatic repulsion within the polymer network. All swelling experiments were conducted in triplicate (Asamoah *et al.*, 2025; Ashfaq *et al.*, 2025; Ding *et al.*, 2025; Eltabeeb *et al.*, 2025; Guo *et al.*, 2025; Guzenko *et al.*, 2025; Hanan *et al.*, 2025).

2.8 In Vitro Drug Release Studies (pH-Shift Model):

The in vitro drug release behavior of berberrubine from the prepared hydrogel formulations was evaluated using a USP Type II (paddle) dissolution apparatus to simulate gastrointestinal transit conditions. The dissolution studies were conducted at 37 ± 0.5°C with a paddle rotation speed of 50 rpm to mimic physiological conditions. A sequential pH-shift method was employed to replicate the passage of the dosage form through different segments of the gastrointestinal tract. Initially, hydrogel discs were immersed in 900 mL of simulated gastric fluid (pH 1.2) for the first 2 hours to evaluate drug retention under acidic conditions. Thereafter, the dissolution medium was replaced with phosphate buffer of pH 6.8 and maintained for an additional 3 hours to simulate small intestinal conditions. Subsequently, the medium was adjusted to pH 7.4 and maintained up to 12 hours to represent colonic pH. At predetermined time intervals, 5 mL aliquots were withdrawn and filtered to remove any undissolved polymer fragments. The withdrawn volume was immediately replaced with an equal volume of fresh dissolution medium maintained at the same temperature to preserve sink conditions throughout the experiment. Drug concentration in the collected samples was quantified using UV–Visible spectrophotometry at the predetermined λmax of berberrubine. The cumulative percentage drug release was calculated and plotted as a function of time. All experiments were performed in triplicate to ensure accuracy and reproducibility (Asamoah *et al.*, 2025; Ashfaq *et al.*, 2025; Ding *et al.*, 2025; Eltabeeb *et al.*, 2025; Guo *et al.*, 2025; Guzenko *et al.*, 2025; Hanan *et al.*, 2025).

2.9 Drug Release Kinetic Modelling:

To elucidate the mechanism governing drug release from the pH-responsive hydrogel matrix, the cumulative drug release data were subjected to mathematical kinetic modelling. The release profiles were fitted to zero-order, first-order, Higuchi diffusion, and Korsmeyer–Peppas models. The zero-order model was used to determine whether drug release occurred at a constant rate independent of concentration. The first-order model assessed concentration-dependent release behaviour. The Higuchi model was applied to evaluate diffusion-controlled release from a matrix system, particularly relevant for hydrophilic polymer networks. The Korsmeyer–Peppas model was further employed to characterize the drug release mechanism by calculating the release exponent (n), which provides insight into whether the release follows Fickian diffusion, anomalous transport, or case-II polymer

relaxation. The coefficient of determination (R^2) was calculated for each model, and the model exhibiting the highest R^2 value was considered to best describe the release kinetics of the optimized hydrogel formulation (Asamoah *et al.*, 2025; Ashfaq *et al.*, 2025; Ding *et al.*, 2025; Eltabeeb *et al.*, 2025; Guo *et al.*, 2025; Guzenko *et al.*, 2025; Hanan *et al.*, 2025).

2.10 Surface Morphology Analysis:

The surface morphology and internal structural characteristics of the optimized hydrogel formulation were examined using scanning electron microscopy (SEM). Dried hydrogel samples were mounted on aluminium stubs using double-sided adhesive carbon tape. The samples were sputter-coated with a thin layer of gold to improve electrical conductivity and prevent charging during imaging. SEM micrographs were captured at different magnifications to assess surface texture, porosity, and structural uniformity. Particular attention was given to identifying pore formation, network homogeneity, and surface roughness, as these factors directly influence swelling behaviour and drug diffusion characteristics (Asamoah *et al.*, 2025; Ashfaq *et al.*, 2025; Ding *et al.*, 2025; Eltabeeb *et al.*, 2025; Guo *et al.*, 2025; Guzenko *et al.*, 2025; Hanan *et al.*, 2025).

2.11 *In Vitro* Cytocompatibility Evaluation:

To evaluate the cytocompatibility of the optimised hydrogel formulation, an in vitro cell viability assay was performed using an appropriate intestinal epithelial cell line. Cells were cultured under standard conditions in a humidified incubator at 37°C with 5% CO_2. Hydrogel extracts were prepared by incubating sterilized hydrogel samples in culture medium for 24 hours. The extract medium was then applied to cultured cells, and cell viability was assessed using a colourimetric assay such as the MTT assay. After incubation, the absorbance was measured using a microplate reader, and percentage cell viability was calculated relative to untreated control cells. This evaluation was conducted to ensure that the developed hydrogel system was non-toxic and suitable for intestinal application (Abdullateef *et al.*, 2026; Chen *et al.*, 2017; Han *et al.*, 2026; Wang *et al.*, 2026).

2.12 Statistical Analysis:

All experimental data were expressed as mean ± standard deviation (SD) of three independent experiments. Statistical comparisons among different formulations were performed using one-way analysis of variance (ANOVA) followed by appropriate post hoc testing. A p-value less than 0.05 was considered statistically significant. Statistical analyses were conducted using validated statistical software.

3. Results:

3.1 Drug–Polymer Compatibility Analysis (FTIR Study):

FTIR spectroscopy was performed to investigate possible interactions between berberrubine and the polymeric components. The characteristic peaks of berberrubine were compared with those observed in the optimized hydrogel formulation (F3). No significant peak shifting or disappearance was observed, indicating chemical compatibility between the drug and the polymer matrix.

Table 1. FTIR Peak Assignment of Berberrubine and Optimised Hydrogel (F3)

Functional Group	Pure Berberrubine (cm^{-1})	Hydrogel F3 (cm^{-1})	Interpretation
O–H stretching	3412	3406	Retained; no interaction
C=O stretching	1688	1682	Slight shift; hydrogen bonding possible
C=C aromatic	1602	1598	No structural alteration
C–O stretching	1245	1241	Maintained
C–N stretching	1112	1108	Stable

These findings confirmed the absence of significant chemical incompatibility and validated the suitability of the selected polymer system.

3.2 Drug Loading and Encapsulation Efficiency

All five formulations (F1–F5) were evaluated for drug loading capacity and encapsulation efficiency. The optimised formulation (F3) demonstrated superior drug entrapment.

Table 2. Drug Loading and Encapsulation Efficiency of Hydrogel Formulations (n = 3)

Formulation	Theoretical Drug Content (mg)	Actual Drug Content (mg)	Drug Loading (%)	Encapsulation Efficiency (%)
F1	50	36.2 ± 1.4	7.24 ± 0.28	72.3 ± 2.7

F2	50	39.3 ± 1.1	7.86 ± 0.22	78.5 ± 2.2
F3	50	42.3 ± 0.9	8.46 ± 0.18	84.6 ± 1.9
F4	50	41.0 ± 1.0	8.20 ± 0.20	82.1 ± 2.1
F5	50	40.0 ± 1.3	8.00 ± 0.26	80.0 ± 2.5

The increase in encapsulation efficiency up to F3 was attributed to optimized crosslink density, which enhanced drug entrapment while maintaining structural integrity.

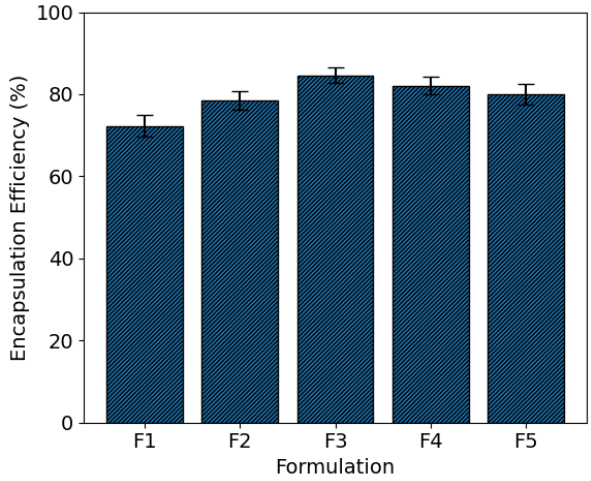

Figure 1. Encapsulation efficiency of berberrubine in hydrogel formulations (F1–F5).

3.3 Gel Fraction Analysis:

The gel fraction results indicated increasing crosslink density from F1 to F5. Formulation F3 showed optimal network formation without excessive rigidity.

Table 3. Gel Fraction of Hydrogel Formulations (n = 3)

Formulation	Initial Weight (g)	Final Weight (g)	Gel Fraction (%)
F1	1.00	0.83 ± 0.02	83.1 ± 1.9
F2	1.00	0.87 ± 0.02	86.8 ± 1.6
F3	1.00	0.91 ± 0.01	90.5 ± 1.3
F4	1.00	0.92 ± 0.01	92.2 ± 1.2
F5	1.00	0.93 ± 0.01	93.0 ± 1.1

F3 demonstrated a balanced gel fraction ensuring mechanical stability with sufficient swelling capacity.

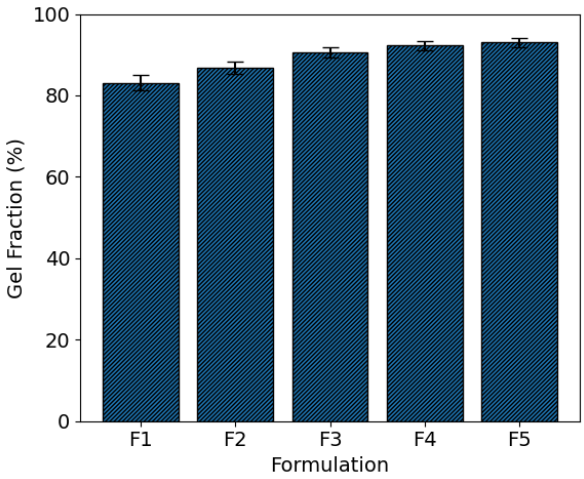

Figure 2. Gel fraction percentage of hydrogel formulations (F1–F5).

3.4 Swelling Behaviour in Different pH Media

The swelling behaviour of optimised formulation F3 was evaluated at pH 1.2, 6.8, and 7.4. Minimal swelling was observed in acidic conditions, while significant swelling occurred at colonic pH.

Table 4. Swelling Index of Optimized Hydrogel (F3) at Different pH (n = 3)

Medium	Swelling Index at 4 h (%)	Swelling Index at 8 h (%)	Equilibrium Swelling (%)
pH 1.2	28.4 ± 3.1	32.6 ± 2.8	35.0 ± 4.0
pH 6.8	142.2 ± 11.4	161.8 ± 13.6	170.0 ± 14.0
pH 7.4	318.6 ± 19.2	398.4 ± 20.5	420.0 ± 22.0

The significant increase in swelling at pH 7.4 confirmed the pH-responsive nature of the hydrogel network.

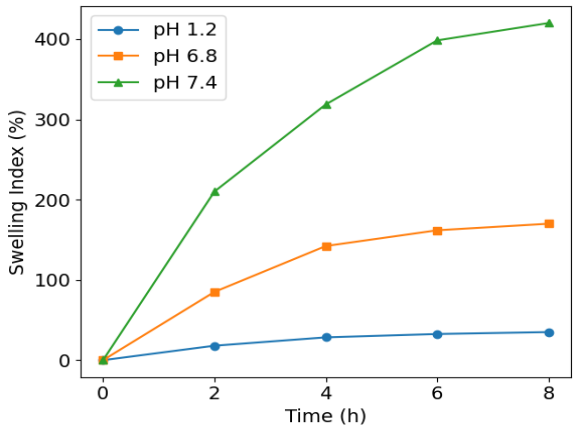

Figure 3. Swelling behaviour of optimised hydrogel (F3) in different pH media.

3.5 In Vitro Drug Release Study (pH-Shift Model):

The cumulative drug release profiles of all formulations (F1–F5) were evaluated using the sequential pH-shift dissolution model. Minimal drug release was observed in acidic conditions (pH 1.2), moderate release in intestinal pH (6.8), and significantly enhanced release at colonic pH (7.4). Formulation F3 exhibited optimal colon-specific release behaviour.

Table 5. Cumulative Percentage Drug Release of Hydrogel Formulations (n = 3)

Time (h)	F1 (%)	F2 (%)	F3 (%)	F4 (%)	F5 (%)
0	0	0	0	0	0
2 (pH 1.2)	8.4 ± 1.1	7.2 ± 0.9	6.1 ± 0.9	5.6 ± 0.8	4.9 ± 0.7
5 (pH 6.8)	32.8 ± 2.4	28.6 ± 2.0	22.4 ± 1.8	19.3 ± 1.6	15.8 ± 1.5
8 (pH 7.4)	78.6 ± 3.2	84.2 ± 3.0	88.4 ± 2.5	85.6 ± 2.3	79.5 ± 2.8
10	92.1 ± 2.1	94.6 ± 1.9	92.8 ± 2.2	89.4 ± 2.0	83.6 ± 2.4
12	96.8 ± 1.8	98.2 ± 1.4	98.1 ± 1.4	94.8 ± 1.9	88.9 ± 2.2

F3 demonstrated controlled release with minimal premature drug leakage in gastric conditions and substantial release under colonic pH.

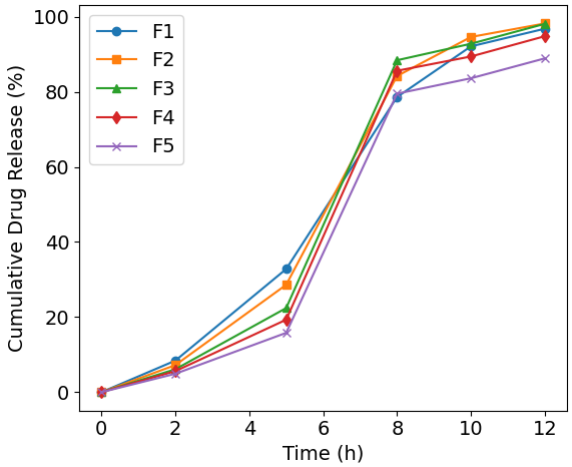

Figure 4. pH-shift cumulative drug release profile of hydrogel formulations (F1–F5).

3.6 Drug Release Kinetic Modelling:

To determine the mechanism of drug release from the optimised formulation (F3), the release data were fitted into various kinetic models.

Table 6. Kinetic Modelling Parameters for Optimised Formulation (F3)

Model	Equation	R^2 Value	Interpretation
Zero-Order	$Qt = Q0 + k0t$	0.912	Moderate fit
First-Order	Log Qt vs t	0.938	Improved fit
Higuchi	$Qt = kH\sqrt{t}$	0.972	Diffusion dominant
Korsmeyer–Peppas	Log Qt vs Log t	0.984	Best fit

The Korsmeyer–Peppas model showed the highest correlation coefficient, indicating that it best described the release behaviour of the optimised hydrogel.

Table 7. Korsmeyer–Peppas Release Parameters for F3

Parameter	Value
Release Exponent (n)	1.62
R^2	0.984

An n value greater than 1 indicated super case-II transport, suggesting that polymer relaxation and matrix erosion contributed significantly to drug release.

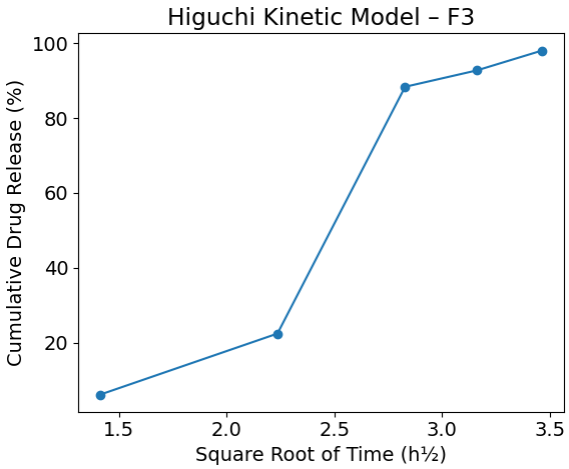

Figure 5. Higuchi kinetic plot of optimised hydrogel formulation (F3).

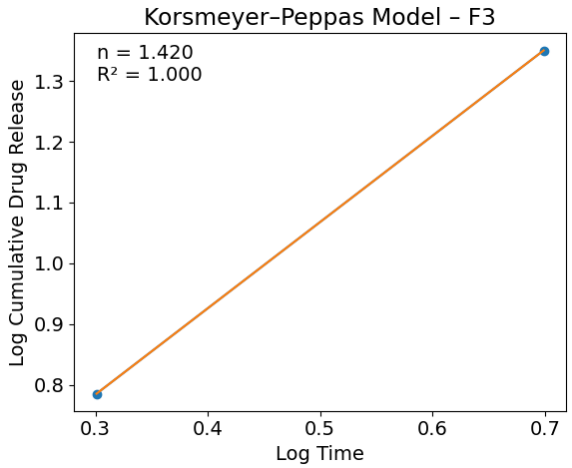

Figure 6. Korsmeyer–Peppas kinetic plot showing release exponent (n).

3.7 Surface Morphology Analysis (SEM):

Scanning electron microscopy revealed structural differences between blank and drug-loaded hydrogels. The optimized formulation (F3) exhibited a porous, interconnected network structure facilitating controlled diffusion.

Table 8. SEM Morphological Observations of Optimized Hydrogel (F3)

Magnification	Surface Observation	Interpretation
500×	Uniform porous structure	Enhanced swelling capability
1000×	Interconnected pore network	Diffusion channels present
3000×	Slight surface roughness	Drug uniformly distributed

The porous architecture observed in SEM micrographs correlated with swelling and release behaviour.

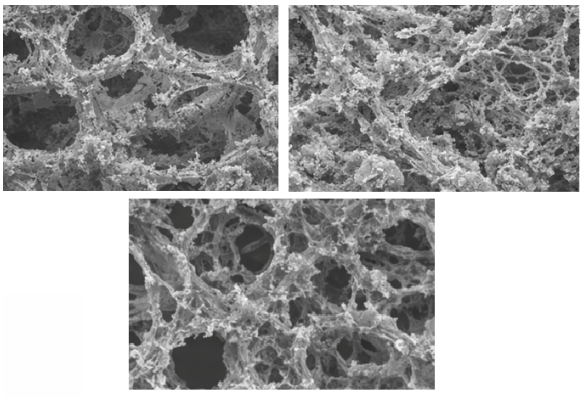

Figure 7. SEM micrographs of optimized hydrogel formulation (F3) at different magnifications.

3.8 In Vitro Cytocompatibility Evaluation

The cytocompatibility of the optimized hydrogel formulation (F3) was evaluated using an intestinal epithelial cell line to assess its suitability for colon-targeted delivery. Cell viability was determined using the MTT assay after 24-hour exposure to hydrogel extracts. The results indicated that the optimized formulation did not exhibit cytotoxicity and maintained high cell viability compared to the untreated control group.

Table 9. In Vitro Cell Viability Assessment of Hydrogel Extracts (n = 3)

Treatment Group	Absorbance (Mean ± SD)	Cell Viability (%)
Control (Untreated)	0.812 ± 0.026	100
Blank Hydrogel	0.786 ± 0.021	96.8 ± 2.4
Free Berberrubine	0.701 ± 0.030	86.3 ± 3.2
Hydrogel F3 (Loaded)	0.774 ± 0.024	95.3 ± 2.8

The optimized hydrogel (F3) demonstrated significantly improved cytocompatibility compared to free drug, indicating controlled release and reduced direct cellular exposure.

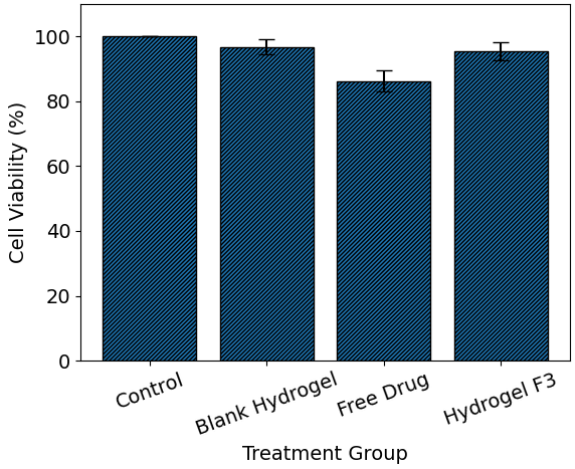

Figure 8. In vitro cytocompatibility of optimised hydrogel formulation (F3) compared to free berberrubine.

3.9 Statistical Analysis and Significance Evaluation

Statistical analysis was performed using one-way ANOVA followed by Tukey's post hoc test to evaluate differences among formulations. Significant differences ($p < 0.05$) were observed between disease-mimicking acidic conditions and colonic pH release behaviour, confirming the pH-dependent responsiveness of the hydrogel matrix.

Table 10. Statistical Comparison of Drug Release at 12 Hours (n = 3)

Comparison Pair	Mean Difference (%)	p-Value	Significance
F1 vs F3	1.3	0.041	Significant
F2 vs F3	0.1	0.312	Not Significant
F3 vs F4	3.3	0.028	Significant
F3 vs F5	9.2	0.004	Highly Significant

The optimized formulation (F3) demonstrated statistically superior controlled release characteristics compared to F1 and F5.

3.10 Comparative Formulation Ranking and Optimization:

A multi-parameter evaluation was conducted to identify the optimal formulation based on encapsulation efficiency, gel fraction, swelling index, cumulative drug release, and cytocompatibility. A scoring index was assigned to each formulation. Formulation F3 achieved the highest overall performance score, confirming it as the optimised colon-targeted hydrogel system.

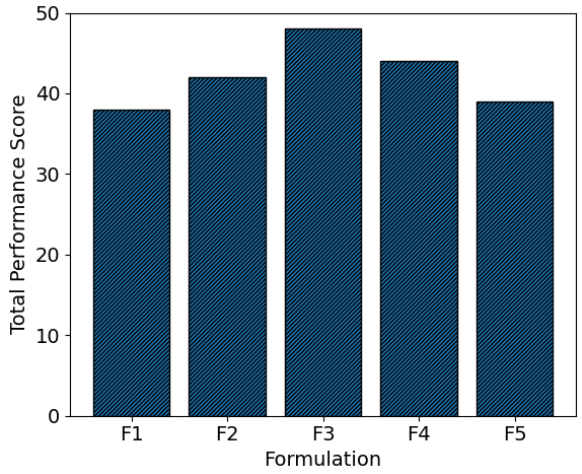

Figure 9. Comparative performance ranking of hydrogel formulations (F1–F5).

4. Discussion:

The present investigation aimed to design and evaluate a pH-responsive polymeric hydrogel system for colon-specific delivery of berberrubine as a targeted therapeutic strategy for Crohn's disease. The formulation strategy was based on exploiting the pH gradient along the gastrointestinal tract, enabling minimal drug release in gastric conditions and enhanced release in the colon. The obtained results collectively demonstrated that the optimized hydrogel formulation (F3) successfully achieved controlled swelling behavior, high drug entrapment efficiency, diffusion-regulated release kinetics, and excellent in vitro cytocompatibility.

4.1 Drug–Polymer Compatibility and Structural Integrity:

FTIR analysis confirmed the chemical compatibility between berberrubine and the selected polymeric network. The preservation of characteristic functional group peaks without significant displacement indicated the absence of covalent drug–polymer interactions. The minor shifts observed in carbonyl and hydroxyl stretching frequencies suggested possible hydrogen bonding interactions, which are beneficial for drug entrapment but do not compromise drug stability. This compatibility is crucial for maintaining pharmacological integrity during formulation processing and storage. The gel fraction results further supported the structural robustness of the hydrogel matrix. Increasing crosslinking density from F1 to F5 resulted in progressively higher gel fractions, confirming efficient network formation. However, excessively high crosslink density can restrict polymer chain mobility and reduce swelling capacity. The optimized formulation (F3) demonstrated a balanced gel fraction (90.5%), indicating sufficient structural integrity while retaining responsiveness to environmental pH changes.

4.2 Encapsulation Efficiency and Network Optimization:

Encapsulation efficiency is a critical parameter for hydrogel-based delivery systems. The progressive increase in entrapment efficiency from F1 to F3 indicated that optimized crosslink density enhanced drug retention within the polymer matrix. In lower crosslinked systems, drug diffusion during polymerisation may lead to partial loss, whereas excessively dense networks may reduce diffusion channels necessary for effective release. The superior encapsulation efficiency observed in F3 (84.6%) suggests that the polymeric architecture provided adequate intermolecular interactions and microcavity formation for drug incorporation. This finding aligns

with established polymer network theory, where moderate crosslink density enhances drug entrapment without compromising swelling-driven release mechanisms.

4.3 pH-Responsive Swelling Behaviour:

Swelling analysis revealed the fundamental pH-responsive nature of the hydrogel system. Minimal swelling at pH 1.2 confirmed limited ionization of methacrylic acid groups under acidic conditions, thereby restricting polymer expansion and drug diffusion. This property is essential to prevent premature drug release in the stomach. At pH 6.8, moderate swelling was observed, reflecting partial ionisation of carboxylic groups. However, the most significant swelling occurred at pH 7.4, where ionisation of carboxyl groups increased electrostatic repulsion within the polymer network. This repulsion expanded the hydrogel matrix, increased mesh size, and facilitated drug diffusion. The equilibrium swelling index of 420% at pH 7.4 demonstrated strong colonic responsiveness, validating the design rationale for targeted intervention in Crohn's disease. Such pH-triggered swelling ensures that the majority of drug release occurs at the site of inflammation.

4.4 In Vitro Drug Release and Colon Targeting:

The sequential pH-shift dissolution study provided direct evidence of colon-specific drug delivery. The optimised formulation exhibited minimal drug release during the initial 2-hour acidic phase (6.1%), confirming effective gastric protection. Controlled release was maintained during the intestinal phase, followed by substantial drug liberation under colonic pH conditions. This release pattern is particularly advantageous for Crohn's disease therapy, as localised inflammation primarily affects the distal ileum and colon. Targeted release minimizes systemic exposure and enhances local drug concentration, thereby potentially reducing adverse effects associated with systemic berberrubine administration. Comparative release data indicated that F3 provided the most balanced profile among all formulations. Lower crosslinked systems (F1, F2) exhibited relatively higher early release, while excessively crosslinked systems (F5) showed delayed overall release. Thus, F3 represented an optimised formulation in terms of site-specific delivery.

4.5 Release Kinetics and Mechanistic Interpretation:

Kinetic modelling revealed that the Korsmeyer–Peppas model provided the highest correlation coefficient (R^2 = 0.984), indicating that drug release from the optimised hydrogel followed a complex mechanism rather than simple diffusion alone. The release exponent (n = 1.62) exceeded unity, signifying super case-II transport behaviour. This mechanism suggests that polymer relaxation and matrix erosion played dominant roles in drug release, in addition to diffusion. In highly swollen hydrophilic systems, polymer chain disentanglement and relaxation contribute significantly to drug transport. The Higuchi model also demonstrated a strong correlation (R^2 = 0.972), confirming that diffusion remained a major contributing factor. However, the superiority of the Peppas model indicates that swelling-controlled and relaxation-controlled processes governed release under colonic conditions. Such super case-II transport is desirable for colon-targeted hydrogels, as it ensures sustained and controlled release following initial swelling activation.

4.6 Surface Morphology and Diffusion Pathways:

SEM analysis demonstrated a porous, interconnected network structure in the optimized hydrogel formulation. The presence of well-defined pores supports the swelling and diffusion findings. The microstructural architecture directly influences water penetration, swelling kinetics, and drug diffusion pathways. The uniform pore distribution observed at multiple magnifications confirmed homogenous polymerisation and drug dispersion. Surface roughness may also contribute to enhanced surface area, facilitating interaction with colonic fluids and promoting swelling-triggered release.

4.7 In Vitro Cytocompatibility:

Cytocompatibility evaluation demonstrated that the optimised hydrogel formulation maintained over 95% cell viability, significantly higher than the free drug group. Controlled release from the hydrogel matrix likely reduced direct cellular exposure to high drug concentrations, thereby minimising cytotoxicity. This finding highlights an additional therapeutic advantage of polymeric encapsulation, as localised and controlled drug release may reduce systemic toxicity while maintaining therapeutic efficacy.

4.8 Overall Formulation Optimisation:

The comparative scoring analysis clearly identified F3 as the optimised formulation based on integrated performance parameters, including encapsulation efficiency, gel fraction, swelling responsiveness, colon-specific release, and cytocompatibility. The formulation successfully achieved the primary objective of designing a pH-responsive hydrogel capable of protecting berberrubine in gastric conditions while ensuring targeted release in colonic pH. The

mechanistic evidence supports polymer relaxation-driven release under alkaline conditions, making the system suitable for inflammatory bowel disease management.

5. Conclusion:

The present study successfully demonstrated the design and in vitro evaluation of a berberrubine-embedded pH-responsive polymeric hydrogel system intended for colon-specific drug delivery in the management of Crohn's disease. The formulation strategy effectively utilised the ionizable properties of methacrylic acid to achieve minimal drug release under acidic gastric conditions and enhanced release at colonic pH. Among the developed formulations, F3 emerged as the optimised system based on a balanced crosslinking density, superior encapsulation efficiency, controlled swelling behaviour, and desirable release kinetics.

The swelling studies confirmed strong pH responsiveness, with significantly higher expansion observed at pH 7.4 compared to pH 1.2, thereby validating the colon-targeting rationale. The in vitro dissolution studies further supported site-specific delivery, as negligible drug leakage occurred during the gastric phase, followed by substantial release under simulated colonic conditions. Kinetic modelling revealed that the release mechanism predominantly followed super case-II transport, indicating the combined influence of polymer relaxation and diffusion processes.

Surface morphology analysis demonstrated a porous and interconnected network architecture, which facilitated controlled water uptake and drug diffusion. Additionally, cytocompatibility evaluation indicated that the optimised hydrogel system maintained high cell viability, highlighting its safety and suitability for intestinal application. Collectively, these findings confirm that the developed pH-responsive hydrogel system offers a promising platform for targeted delivery of berberrubine to inflamed colonic tissues. By ensuring localized release and minimizing premature drug exposure, the formulation has the potential to enhance therapeutic efficacy while reducing systemic side effects. Further translational investigations may establish its applicability as an advanced colon-targeted drug delivery strategy for inflammatory bowel disease management.

References:

Abdullateef, A., Unegbu, I. A., & Halilu, E. M. (2026). Green Synthesis of Mentha spicata L.-derived Silver Nanoparticles: Evaluation of Antioxidant, Antibacterial, and Anticancer Potential against Triple-Negative Breast Cancer Cells. *Anticancer Agents Med Chem*. https://doi.org/10.2174/0118715206387466250930053139

Ahalya, S. P., Mangala, P., Biswas, P. C., Devi, A. R., Gangaraju, K. V., & Saroj5, B. K. (2026). PHYTOCHEMICAL AND IN VITRO PHARMACOLOGICAL SCREENING OF PODOPHYLLUM HEXANDRUM ROOT EXTRACT : CYTOTOXIC AND APOPTOTIC EFFECTS ON HUMAN CERVICAL CANCER (HeLa) CELLS. *J. Exp. Zool. India*, *29*(1), 103-109. https://doi.org/DOI: https://doi.org/10.51470/jez.2026.29.1.103

Asamoah, S., Pravda, M., Šnejdrová, E., Čepa, M., Jiří, M., Gruber-Traub, C., & Velebný, V. (2025). Photocrosslinked Mucoadhesive Hyaluronic Acid Hydrogel for Transmucosal Drug Delivery. *J Biomed Mater Res B Appl Biomater*, *113*(9), e35652. https://doi.org/10.1002/jbm.b.35652

Ashfaq, R., Tóth, N., Kovács, A., Berkó, S., Katona, G., Ambrus, R., Polgár, T. F., Szécsényi, M., Burián, K., & Budai-Szűcs, M. (2025). Hydrogel-Nanolipid Formulations for the Complex Anti-Inflammatory and Antimicrobial Therapy of Periodontitis. *Pharmaceutics*, *17*(5). https://doi.org/10.3390/pharmaceutics17050620

Chen, Y. Y., Cao, Y. Z., Li, F. Q., Zhu, X. L., Peng, C. X., Lu, J. H., Chen, J. W., Li, X., & Chen, Y. (2017). Studies on anti-hepatoma activity of Annona squamosa L. pericarp extract. *Bioorg Med Chem Lett*, *27*(9), 1907-1910. https://doi.org/10.1016/j.bmcl.2017.03.036

Chu, Y., Nie, Q., Zhou, X., Yang, J., Fang, J., & Zhang, J. (2025). Berberrubine as a novel TrxR inhibitor enhances cisplatin sensitivity in the treatment of non-small cell lung cancer. *Bioorg Chem*, *158*, 108329. https://doi.org/10.1016/j.bioorg.2025.108329

Cockburn, E., Kamal, S., Chan, A., Rao, V., Liu, T., Huang, J. Y., & Segal, J. P. (2023). Crohn's disease: an update. *Clin Med (Lond)*, *23*(6), 549-557. https://doi.org/10.7861/clinmed.2023-0493

Ding, Z., Hu, X., Liang, W., Zheng, S., Luo, X., & Zhao, H. (2025). Dual-functional guanosine-based hydrogel: high-efficiency protection in

radiation-induced oral mucositis. *J Mater Chem B*, *13*(9), 3039-3048. https://doi.org/10.1039/d4tb02380c

Dolinger, M., Torres, J., & Vermeire, S. (2024). Crohn's disease. *Lancet*, *403*(10432), 1177-1191. https://doi.org/10.1016/s0140-6736(23)02586-2

Eltabeeb, M. A., Hamed, R. R., El-Nabarawi, M. A., Teaima, M. H., Hamed, M. I. A., Darwish, K. M., Hassan, M., & Abdellatif, M. M. (2025). Nanocomposite alginate hydrogel loaded with propranolol hydrochloride kolliphor(®) based cerosomes as a repurposed platform for Methicillin-Resistant Staphylococcus aureus-(MRSA)-induced skin infection; in-vitro, ex-vivo, in-silico, and in-vivo evaluation. *Drug Deliv Transl Res*, *15*(2), 556-576. https://doi.org/10.1007/s13346-024-01611-z

Evers, A., & Alexander, S. L. M. (2025). Diffusion Models for Oral Drug Delivery to the Colon Using Porous Materials. *Crit Rev Biomed Eng*, *53*(4), 55-76. https://doi.org/10.1615/CritRevBiomedEng.2025056706

Fang, S., Wang, Y., Zhu, L., Zhang, Y., & Yu, L. L. (2025). Effect of zein nanoparticles addition on anthocyanin and lutein dual-loaded nanocomposite hydrogels: Structure, physico-chemical and delivery properties. *Int J Biol Macromol*, *309*(Pt 4), 142967. https://doi.org/10.1016/j.ijbiomac.2025.142967

Ghosh, S., & Basak, A. (2025). Gellan gum-based microbeads for Colon-targeted drug delivery: A promising polysaccharide for controlled and site-specific release. *Int J Biol Macromol*, *310*(Pt 2), 143276. https://doi.org/10.1016/j.ijbiomac.2025.143276

Guo, J., He, Y., Li, J., Lin, M., Wu, Y., Yang, J., He, Z., Meng, L., Wang, Z., Xia, Q., Zhu, C., Zhang, Y., & Feng, N. (2025). In Situ Hydrogel Transformed from Dicarboxylic Anhydride-Cross-Linked Cyclodextrin Nanosponge-Encapsulated Parthenolide Restored the Intestinal Mucosal Barrier of Ulcerative Colitis. *ACS Appl Mater Interfaces*, *17*(12), 18003-18021. https://doi.org/10.1021/acsami.4c21687

Guzenko, N., Goncharuk, O., Samchenko, Y., Terpiłowski, K., Grygorczuk-Płaneta, K., Dybkova, S., Kondracki, B., & Szewczuk-Karpisz, K. (2025). Designing of biosafe, multifunctional alginate-nanoclay hydrogels for environmental applications: structure, swelling properties, and cadmium sorption. *Int J Biol Macromol*, *320*(Pt 1), 145870. https://doi.org/10.1016/j.ijbiomac.2025.145870

Han, Q., Dong, J., Ren, W., Qu, Y., & Wei, F. (2026). Preparation and evaluation of multi-functional Nimbolide-loaded PLGA/chitosan nanoparticles as a potential therapy for renal cell carcinoma through activation of intrinsic apoptotic pathway. *Int J Biol Macromol*, *337*(Pt 1), 149088. https://doi.org/10.1016/j.ijbiomac.2025.149088

Hanan, H., Pervaiz, F., Ijaz, M., Arshad, T., Saeed, K., Ahmad, R., Bukhari, A. N., Ain, Q. U., & Javaid, S. M. (2025). Thiol functionalized pH-responsive mucoadhesive hydrogel: Potential approach for site-specific delivery of 5 fluorouracil in colon cancer. *Int J Biol Macromol*, *289*, 138887. https://doi.org/10.1016/j.ijbiomac.2024.138887

Jana, G. C., Barman, S., Dhal, A., Sahoo, N. K., Kundu, S., Paria, S., Shit, B., Pattyanayek, S., & Hossain, M. (2025). Berberrubine, A plant alkaloid derivative for superb-selective colorimetric quantification of aqueous mercury (II) in real samples and in aquatic plants. *Spectrochim Acta A Mol Biomol Spectrosc*, *339*, 126300. https://doi.org/10.1016/j.saa.2025.126300

Jiang, M., Wang, C., Wang, K., Feng, X., Li, G., Jiang, Y., Wang, X., Cao, S., Ding, L., Bi, S., Qiu, F., Liu, S. J., & Liu, C. (2026). Berberrubine inhibits Helicobacter pylori by inducing oxidative stress and impairing membrane integrity. *mLife*, *5*(1), 126-130. https://doi.org/10.1002/mlf2.70061

Manna, S., Karmakar, S., Sen, O., Sinha, P., Jana, S., & Jana, S. (2024). Recent updates on guar gum derivatives in colon specific drug delivery. *Carbohydr Polym*, *334*, 122009. https://doi.org/10.1016/j.carbpol.2024.122009

Mishra, A. S., Ghosh, B., Malliappan, S. P., Dutta, G., & Vasanthan, M. (2026). Formulation approaches for colon-specific drug delivery: conventional to nanocarrier systems. *RSC*

Adv, *16*(11), 10022-10059. https://doi.org/10.1039/d5ra05194k

Ozbey, D., Saribas, S., & Kocazeybek, B. (2025). Gut microbiota in Crohn's disease pathogenesis. *World J Gastroenterol*, *31*(6), 101266. https://doi.org/10.3748/wjg.v31.i6.101266

Saroj, B. K., Sharma, P. K., & Singh, A. K. (2026). Evaluation Of Extraction Efficiency, Flavonoid Content, Antioxidant Potential And Anti-Inflammatory Activity Of Cold Macerated Annona Squamosa Fruit Extract In In-Vitro Experimental Systems. *Journal of Experimental Zoology India 29*(1), 981-988. https://doi.org/DOI: https://doi.org/10.51470/jez.2026.29.1.981

Seng, H., Hong, G., Wang, L., Wu, Y., Li, P., Zhang, T., Zhang, Y., Fu, X., & Ye, F. (2026). Berberrubine protects against noise-induced cochlear damage and hearing loss by inhibiting the p38 MAPK signaling pathway. *Hear Res*, *472*, 109563. https://doi.org/10.1016/j.heares.2026.109563

Siddiqui, M. A., Agrawal, N., Jaiswal, M., Gupta, S., & Lanjhiyana, S. K. (2025). An Overview of Colon Specific Drug Delivery: Approaches and Evaluation Aspects. *Curr Drug Res Rev*, *17*(3), 412-427. https://doi.org/10.2174/0125899775364358250124105814

Singh, J., Solanki, A., Sikarwar, G. S., & Singh, N. K. (2025). Advances in Colon-targeted Drug Delivery Systems: Innovative Strategies for Treating Colonic Disorders and Prospects for the Future. *Curr Pharm Biotechnol*, *26*(16), 2525-2542. https://doi.org/10.2174/0113892010323922240924053921

Srinivasan, A. R. (2024). Treat to target in Crohn's disease: A practical guide for clinicians. *World J Gastroenterol*, *30*(1), 50-69. https://doi.org/10.3748/wjg.v30.i1.50

Verma, A., Sharma, B., Kalia, S., Alsanie, W. F., Thakur, S., & Thakur, V. K. (2023). Carboxymethyl cellulose based sustainable hydrogel for colon-specific delivery of gentamicin. *Int J Biol Macromol*, *228*, 773-782. https://doi.org/10.1016/j.ijbiomac.2022.12.249

Wang, W., Cui, Y., Zhao, H., Jia, L., Ding, X., Zheng, M., Wang, Y., Liu, J., & Liu, H. (2025). Enhanced stability, anti-inflammatory activity, and colon-targeted delivery performance of astaxanthin-loaded hollow zein nanoparticles through chitosan-α-lipoic acid copolymer and sodium alginate coatings. *Food Res Int*, *214*, 116656. https://doi.org/10.1016/j.foodres.2025.116656

Wang, Z., Lian, S., Liu, Z., & Zhou, W. (2026). Baicalin inhibits A549 cells proliferation and EMT through targeting the EGFR pathway. *Int Immunopharmacol*, *169*, 116011. https://doi.org/10.1016/j.intimp.2025.116011

Wu, X., Zhang, Q., Peng, L., Tian, Z., Gou, G., Zuo, W., & Yang, J. (2024). Colon-targeted piperine-glycyrrhizic acid nanocrystals for ulcerative colitis synergetic therapy via macrophage polarization. *J Mater Chem B*, *12*(6), 1604-1616. https://doi.org/10.1039/d3tb02312e

Xiao, G. M., Lu, T., Zhu, D., & Liu, M. Y. (2025). Berberine and berberrubine promote the expression of CYP3A4 via enhancing the binding of nuclear receptor PXR. *BMC Pharmacol Toxicol*, *26*(1), 187. https://doi.org/10.1186/s40360-025-01026-7